2nd IFAC Workshop on Automatic Control in Offshore Oil and Gas Production,
May 27-29, 2015, Florianópolis, Brazil

Downhole Pressure Soft-Sensing using Interacting Multiple Modeling ⋆

Bruno F. Riccio * **Alex F. Teixeira** ** **Bruno O. S. Teixeira** *

* *Department of Electronic Engineering, Universidade Federal de Minas Gerais (UFMG), Belo Horizonte, MG, Brazil (e-mail: brunoot@ufmg.br).*
** *Research and Development Center (CENPES), Petróleo Brasileiro S.A. (Petrobras), Rio de Janeiro, RJ, Brazil*

Abstract: In this work we design data-driven soft sensors of downhole pressure for gas-lift oil wells. We employ a two-step procedure. First, discrete-time (N)ARX models are identified offline from historical data. Second, recursive predictions of these multiple models are combined with current measured data (of variables other than the downhole pressure) by means of an interacting bank of (unscented) Kalman filters. We investigate the usage (i) of linear versus nonlinear models and (ii) of models with or without seabed variables in addition to platform variables. Results are validated by means of experimental data from three oil wells.

Keywords: Soft sensors, system identification, interacting multiple models, downhole pressure

1. INTRODUCTION

Soft sensors are predictive mathematical models that infer the values of a given process variable from measurements of other variables (Fortuna et al., 2007). They have been applied in oil industry as an alternative to purely hardware instruments (Domlan et al., 2011; Fujiwara et al., 2012). Two classes of soft sensors can be distinguished, namely, model-driven and data-driven (Kadlec et al., 2009). The former is based on first-principle models, while the latter uses data-driven black-box models. In addition, given that industrial processes are described by nonlinear phenomena, nonlinear models should be the natural choice for developing soft sensors. Alternatively, multiple linear models can be employed.

The downhole pressure is a measurement extremely important for the reservoir and production engineers responsible for an oil field because it is measured close to the perforations and frequently used in the production monitoring, control and optimisation strategies. Nonetheless, maintaining and replacing permanent downhole gauge (PDG) sensors to monitor downhole pressure is a challenging task, especially in offshore oil wells (Eck et al., 1999). Thus, soft-sensing techniques are promising alternatives to monitor the downhole variables.

This paper is a follow-up of (Teixeira et al., 2014). We present the design of two-step data-driven soft sensors to online estimate the downhole pressure of three offshore gas-lift oil wells. First, as in (Pagano et al., 2006), discrete-time linear and nonlinear autoregressive with exogenous inputs ((N)ARX) polynomial models are identified offline using experimental data as in (Aguirre et al., 2005). Two kinds of models are obtained: infinite impulse response (IIR) process models and FIR/IIR observation models. Different configurations of inputs and outputs are tested. Second, interacting multiple model (IMM) filter banks (Bar-Shalom et al., 2001) are implemented, with each linear or unscented Kalman filter ((U)KF) of the banks combining a different pair of process and observation models. That is, local (non)linear "closed-loop" models are combined to yield improved downhole pressure estimates compared to the free-run simulation of a single (open-loop) model. Note that, in our approach, the downhole pressure is assumed to be known only during the system identification step. For practical applications, this is the case after downhole sensor installation, when such sensors are more reliable (Eck et al., 1999).

Two relevant issues are investigated in this paper. First, we evaluate what is the advantage of using nonlinear models compared to linear models as often done in the literature (Yang al., 2012). By doing so, we conjecture that it would be simpler to extend the structure of the linear models obtained for a specific well to other wells, as well as to deal with the retuning of the models to address time-varying dynamics. Second, we evaluate the impact of using seabed auxiliary variables as inputs compared to the case of using only platform variables since measurements of the former are not always available in offshore oil wells.

2. PROCESS DESCRIPTION

Gas lift is one of the artificial lift methods used in deep-water oil wells. A simplified diagram of a gas-lift oil well is shown in Figure 1. Table 1 lists some of the process variables often measured. The process is summarized as follows. High-pressure gas flows through the gas-lift pipeline (riser plus flow line) from the gas-lift header at the platform (tag 4) to the subsea christmas tree where it is injected in annulus between tubing and casing string until it reaches an orifice valve installed downhole in the tubing. The fluid density is then reduced such that the reservoir pressure is high enough to transport the multiphase mix-

⋆ This work was partially supported by Petrobras and CNPq.

Copyright © 2015, IFAC

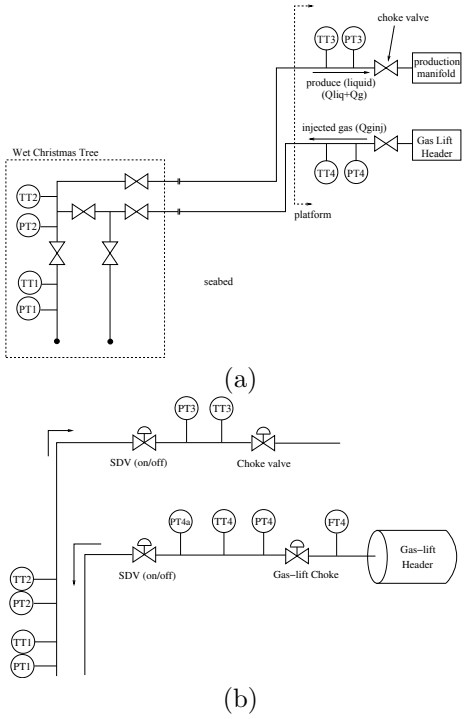

Fig. 1. P&ID diagram of a gas-lifted oil well, where TT and PT are the temperature and pressure transmitters. An overall view is shown in (a), while the platform is detailed in (b). The numbers 1 (downhole) and 2 (wet christmas tree) account for seabed variables, while 3 (production) and 4 (gas lift) account for platform variables. Flow direction is 4-1-2-3. The downhole variables are measured close to the reservoir outlet.

Table 1. Process variables of offshore oil wells.

Tag	Description	Units
PT1	PDG Downhole pressure	kgf/s^2
TT1	PDG Downhole temperature	°C
PT2	Wet christmas tree pressure	kgf/s^2
TT2	Wet christmas tree temperature	°C
PT3a	Pressure before shutdown valve	kgf/cm^2
PT3	Pressure before production choke valve	kgf/cm^2
PT3b	Pressure after production choke valve	kgf/cm^2
TT3	Temperature before production choke valve	°C
FV3	Production choke valve position	%
PT4b	Pressure after gas-lift shutdown valve	kgf/cm^2
PT4a	Pressure before gas-lift shutdown valve	kgf/cm^2
TT4	Temperature before gas-lift shutdown valve	°C
FT4	Instantaneous gas-lift flow rate	m^3/h
FV4	Gas-lift valve position	%
PT4	Pressure after gas-lift choke valve	kgf/cm^2

ture of oil, gas, water to the platform. In the seabed, a set of valves and adapters known as wet christmas tree (PT2 and TT2) control the production flow from seabed to the platform. In the platform, a shutdown valve (PT3a) is available to interrupt the production during an emergency situation and a choke production (PT3 and TT3) valve regulates the production flow rate at the platform. Different flow dynamics are achieved depending on the values of gas-lift (PT4 and PT4a) and downhole (PT1) pressure.

3. METHODOLOGY

We consider the nonlinear dynamic system given by

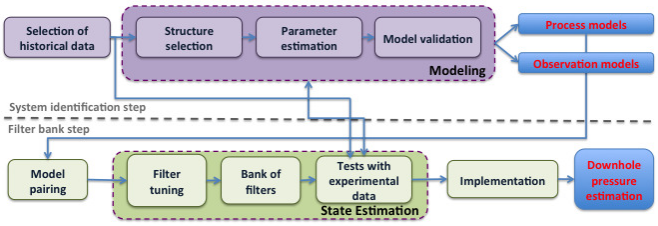

Fig. 2. Diagram of the two-step methodology used to develop downhole pressure soft sensors.

$$x_k = f(x_{k-1}, u^f_{k-1}) + w_{k-1}, \quad (1)$$

$$y_k = h(x_k, u^h_k) + v_k, \quad (2)$$

where $f : \mathbb{R}^n \times \mathbb{R}^{p_f} \longrightarrow \mathbb{R}^n$ is the process model and $h : \mathbb{R}^n \times \mathbb{R}^{p_h} \longrightarrow \mathbb{R}^m$ is the observation model, $x_k \in \mathbb{R}^n$ is the state vector, $y_k \in \mathbb{R}^m$ are measured outputs, $u_k \triangleq \begin{bmatrix} u^f_{k-1} \\ u^h_k \end{bmatrix} \in \mathbb{R}^p$, $p = p_f + p_h$, are known inputs, $w_{k-1} \in \mathbb{R}^n$ and $v_k \in \mathbb{R}^m$ are the zero-mean process noises with covariance Q and R, respectively. Our goal is to obtain state estimates $\hat{x}_{k|k}$ and corresponding covariance $P^{xx}_{k|k}$ that approximate $\mathcal{E}[x_k]$ and $\mathcal{E}[(x_k - \mathcal{E}[x_k])(x_k - \mathcal{E}[x_k])^{\mathrm{T}}]$, respectively, where $\mathcal{E}$ is the expected value. To accomplish that, the two-step procedure illustrated in Figure 2 is employed. In this work, we apply the methodology used in (Teixeira et al., 2014) to develop soft sensors for three oil wells: $W1$, $W2$, and $W3$.

In the system identification step, we assume that a set of dynamical data $\{u_k, x_k, y_k\}$, $k = 1, \ldots, N$, is known. Here, historical data is recovered from a plant information management system (PIMS). Using these offline data, a set of (N)ARX polynomial black-box models $\hat{f}^i$, $i = 1, \ldots, M_f$, and $\hat{h}^j$, $j = 1, \ldots, M_h$, are built independently from each other and rewritten in state space (Aguirre et al., 2005). It is not assumed that such models are globally valid. Here, Q^i and R^j account for the covariance of the one-step-ahead simulation error of $\hat{f}^i$ and $\hat{h}^j$, respectively.

In the filter bank step, we assume that $\{u^s_k, y^s_k\}$, $s = 1, \ldots, M$, are known for all $k > 0$ together with a set of $M \leq M_f M_h$ state-space model pairs $\{\hat{f}^s, \hat{h}^s\}$. For each pair $\{\hat{f}^s, \hat{h}^s\}$, state estimates $\hat{x}^s_{k|k}$ with covariance $P^{xx,s}_{k|k}$ are recursively obtained using M (U)KFs running in parallel. Then, these estimates are combined by an IMM filter bank, yielding $\hat{x}_{k|k}$ and $P^{xx}_{k|k}$ for all $k > 0$ (Bar-Shalom et al., 2001). Note that x is assumed to be known only during the system identification step for a time interval of duration N. For details of the methodology, the reader is referred to (Teixeira et al., 2014).

4. EXPERIMENTAL RESULTS: SYSTEM IDENTIFICATION

In this paper, data from three gas-lift oil wells were used. For each well, different configurations of models were obtained. Table 2 summarizes the main features of all process and observation models that were built.

All (N)ARX polynomial models were built from historical data. All variables listed in Table 1 were sampled at $T =$

Copyright © 2015, IFAC

1min, as the fastest sampling rate provided by the PIMS. Linear and nonlinear autocorrelation analysis (Aguirre, 2005) indicated that such value was appropriate. During modeling, data windows were chosen to include the time intervals for which changes in the operating points are observed, excluding outliers.

Different configurations of inputs and outputs (and corresponding maximum delays) are set for each model. For each model, the one-step-ahead error variance during validation, σ_w^2 or σ_v^2, is calculated. These values are used to set noise covariances Q and R.

Next, for brevity, we present a few (N)ARX polynomial models obtained for the wells $W1$ and $W3$ to illustrate the methodology. All models are listed in Table 2.

4.1 Process models

Consider the following two process models, $W1\_\hat{f}^1$ and $W1\_\hat{f}^4$, built for the well $W1$

$$\begin{aligned} y_1(k) \;=\; & +0.23019\times10^{+1}\, y_1(k-1) - 0.18467\times10^{+1}\, y_1(k-2) \\ & +0.52998\times10^{+0}\, y_1(k-3) + 0.22924\times10^{+1} \\ & +0.24532\times10^{-3}\, u_2(k-4)u_1(k-6) \\ & +0.65057\times10^{-2}\, u_2(k-2)u_1(k-1) \\ & +0.88285\times10^{-3}\, u_2(k-3)u_1(k-3) \\ & -0.87912\times10^{-2}\, u_1(k-1)u_1(k-1) \\ & +0.87217\times10^{-2}\, u_1(k-2)u_1(k-1) \\ & -0.7541\times10^{-2}\, u_2(k-2)u_1(k-2) \\ & +0.30774\times10^{-3}\, u_2(k-1)u_2(k-1) \\ & -0.34288\times10^{-3}\, u_2(k-4)u_2(k-4) \\ & -0.24579\times10^{-4}\, u_1(k-6)u_1(k-3), \end{aligned} \tag{3}$$

$$\begin{aligned} y_1(k) \;=\; & +0.16596\times10^{+1}\, y_1(k-1) - 0.75107\times10^{+0}\, y_1(k-2) \\ & +0.13564\times10^{+2} + 0.23804\times10^{-1}\, u_1(k-4) \\ & -0.20313\times10^{-1}\, u_1(k-2) + 0.10038\times10^{-1}\, u_1(k-3). \end{aligned} \tag{4}$$

Both models have input $\mathrm{TT3}_k$ (u_2 in $W1\_\hat{f}^1$ and u_1 in $W1\_\hat{f}^4$) as the pressure before shutdown valve and output $y_1 = \mathrm{PT1}_k$ as the downhole pressure. $W1\_\hat{f}^1$ also has input $u_1 = \mathrm{TT3}_k$ as the temperature before production choke valve. Note that $W1\_\hat{f}^1$ is a nonlinear model, while $W1\_\hat{f}^4$ is an affine model.

Two process models were built for the well $W3$. $W3\_\hat{f}^1$ is given by

$$\begin{aligned} y_1(k) \;=\; & +0.18394\times10^{+1}\, y_1(k-1) - 0.88832\times10^{+0}\, y_1(k-2) \\ & +0.70988\times10^{+1} - 0.18995\times10^{-1}\, u_1(k-6) \\ & +0.15273\times10^{-1}\, u_1(k-4) + 0.24393\times10^{+0}\, u_2(k-6) \\ & -0.26632\times10^{+0}\, u_2(k-1) - 0.11329\times10^{+0}\, u_2(k-5) \\ & +0.23747\times10^{+0}\, u_2(k-2) - 0.10249\times10^{+0}\, u_2(k-4), \end{aligned} \tag{5}$$

with inputs as the pressure after gas-lift shutdown valve $u_1 = \mathrm{PT4b}_k$ and the temperature before production choke valve $u_2 = \mathrm{TT3}_k$, and with output $y_1 = \mathrm{PT1}_k$ as the downhole pressure. Then, $W3\_\hat{f}^2$ is given by

$$\begin{aligned} y_1(k) \;=\; & +0.18196\times10^{+1}\, y_1(k-1) - 0.86008\times10^{+0}\, y_1(k-2) \\ & +0.10461\times10^{-1}\, u_1(k-9) + 0.57338\times10^{-1}\, u_2(k-1) \\ & +0.27618\times10^{+1} - 0.12367\times10^{-1}\, u_1(k-3) \\ & +0.13539\times10^{-1}\, u_1(k-8) - 0.1631\times10^{-1}\, u_2(k-5), \end{aligned} \tag{6}$$

whose inputs are the wet christmas tree pressure $u_1 = \mathrm{PT2}_k$ and the wet christmas tree temperature $u_2 = \mathrm{TT2}_k$, and output $y_1 = \mathrm{PT1}_k$ is the downhole pressure. Note that model $W3\_\hat{f}^1$ uses only platform variables, while $W3\_\hat{f}^2$ is based on process variables from the seabed.

Model validation for the aforementioned process models is shown in Figure 3a-b. The mean-absolute-percentual error (MAPE) of (3),(4),(5) and (6) are 0,21%, 0,18%, 0,51% and 0,36%, respectively.

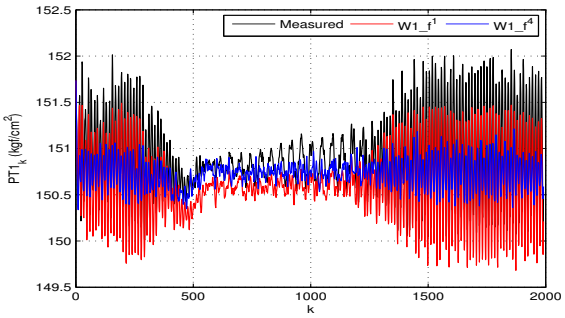

(a)

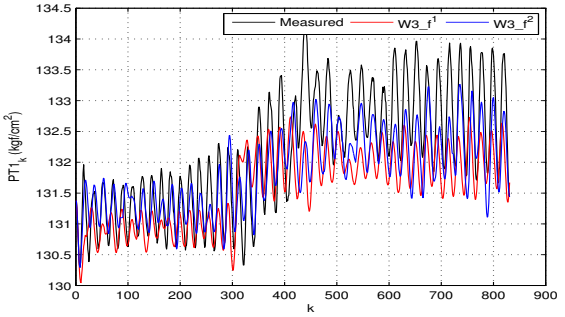

(b)

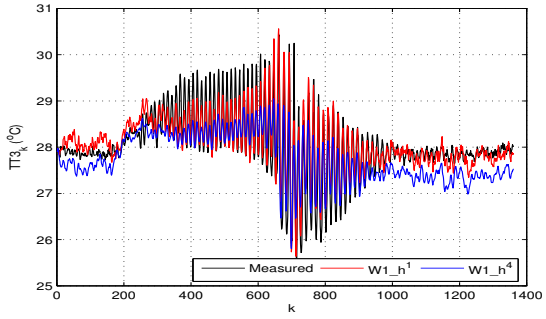

(c)

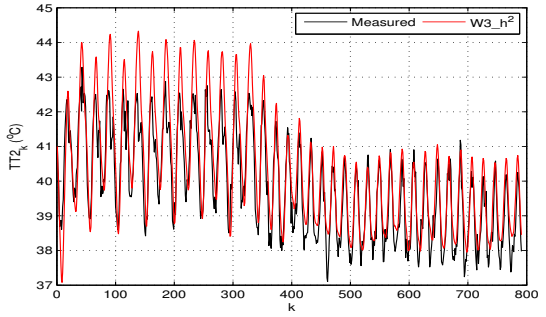

(d)

Fig. 3. Validation of (N)ARX polynomial process and observation models by free-run simulation: (a) $W1\_\hat{f}^1$ (3) and $W1\_\hat{f}^4$ (4), (b) $W3\_\hat{f}^1$ (5) and $W3\_\hat{f}^2$ (6), (c) $W1\_\hat{h}^1$ (7) and $W1\_\hat{h}^4$ (8), and (d) $W3\_\hat{h}^2$ (9).

4.2 Observation models

Next, we show two out of the four observation models built for the well $W1$. $W1\_\hat{h}^1$ and $W1\_\hat{h}^4$ are given by

Copyright © 2015, IFAC

Table 2. Configuration of polynomial (N)ARX models identified for the oil wells $W1$, $W2$ and $W3$, where $\hat{f}$ accounts for process model and $\hat{h}$ for observation model. Polynomial models are characterized by degree ℓ. σ_w^2 and σ_v^2 accounts for one-step-ahead error variance of each model during validation. n_{q^l} and n_z corresponds to the maximum delays of each input or output.

Process models							Observation models						
Tag	ℓ	inputs μ_l	n_{q^l}	output z	n_z	σ_w^2	Tag	ℓ	inputs μ_l	n_{q^l}	output z	n_z	σ_v^2
$W1\_\hat{f}^1$	2	TT3,PT3a	6,4	PT1	3	0,0491	$W1\_\hat{h}^1$	2	PT1,PT3a	3,2	TT3	2	0,2631
$W1\_\hat{f}^2$	2	TT3,PT3a	5,9	PT1	2	0,5349	$W1\_\hat{h}^2$	2	PT1,TT3	2,4	PT3a	3	4,6204
$W1\_\hat{f}^3$	2	TT3,PT3b	4,7	PT1	3	0,5048	$W1\_\hat{h}^3$	2	PT1,PT3a	3,7	TT3	1	0,1028
$W1\_\hat{f}^4$	1	PT3a	4	PT1	2	0,3456	$W1\_\hat{h}^4$	1	PT1,PT3a	1,2	TT3	3	0,2166
$W1\_\hat{f}^5$	1	TT3,PT3a	5,3	PT1	3	0,4315	$W1\_\hat{h}^5$	1	PT1,TT3	3,7	PT3a	2	4,8168
$W1\_\hat{f}^6$	1	TT3,PT3b	7,7	PT1	3	0,3940	$W1\_\hat{h}^6$	1	PT1,PT3a	1,2	TT3	2	0,4016
$W1\_\hat{f}^7$	1	TT3,TT2	5,5	PT1	2	0,1233	$W1\_\hat{h}^7$	1	PT1,PT3a	1,2	TT2	2	0,2267
$W2\_\hat{f}^1$	1	FV4	4	PT1	3	0,2681	$W2\_\hat{h}^1$	1	PT1	2	PT2	2	0,1386
$W2\_\hat{f}^2$	1	FT4	3	PT1	3	0,2664	$W2\_\hat{h}^2$	1	PT1,TT2	2,4	PT2	3	0,1336
$W2\_\hat{f}^3$	1	TT4	4	PT1	3	0,2022							
$W2\_\hat{f}^4$	1	FT4,TT4	3,1	PT1	3	0,2660							
$W3\_\hat{f}^1$	1	PT4b,TT3	6,6	PT1	2	0,2391	$W3\_\hat{h}^1$	1	PT1,PT3a	3,2	TT3	2	0,0214
$W3\_\hat{f}^2$	1	PT2,TT2	9,5	PT1	2	0,2784	$W3\_\hat{h}^2$	1	PT1,PT2	4,3	TT2	3	0,4158

$$\begin{aligned} y_1(k) \;=\; & +0.17061\times10^{-2}\,u_1(k-1)y_1(k-1) \\ & -0.47705\times10^{-2}\,u_1(k-3)y_1(k-2) \\ & -0.19305\times10^{-1}\,u_2(k-2)y_1(k-1) \\ & -0.11265\times10^{+1}\,u_2(k-1)+0.14478\times10^{+1}\,y_1(k-1) \\ & -0.13532\times10^{-2}\,u_2(k-1)u_2(k-1) \\ & +0.16581\times10^{-1}\,u_2(k-2)y_1(k-2) \\ & +0.83789\times10^{-2}\,u_2(k-1)u_1(k-1), \end{aligned} \tag{7}$$

$$\begin{aligned} y_1(k) \;=\; & +0.88732\times10^{+0}\,y_1(k-1)+0.41269\times10^{+0}\,y_1(k-2) \\ & -0.43524\times10^{+0}\,y_1(k-3)+0.30234\times10^{-1}\,u_1(k-1) \\ & -0.36241\times10^{-1}\,u_2(k-2). \end{aligned} \tag{8}$$

Both are multi-input models, with inputs $u_1 = \mathrm{PT1}_k$ as the downhole pressure and $u_2 = \mathrm{PT3a}_k$ as the pressure before shutdown valve, and output given by the temperature before production choke valve $y_1 = \mathrm{TT3}_k$.

One of the observation models built for the well $W3$ is $W3\_\hat{h}^2$, given by

$$\begin{aligned} y_1(k) \;=\; & +0.12471\times10^{+1}\,y_1(k-1)+0.62995\times10^{+0}\,u_1(k-1) \\ & -0.92621\times10^{+0}\,u_1(k-2)-0.189\times10^{-1}\,u_2(k-2) \\ & -0.265\times10^{+0}\,y_1(k-3)+0.98455\times10^{-3}\,u_2(k-3) \\ & +0.31299\times10^{+0}\,u_1(k-4), \end{aligned} \tag{9}$$

whose inputs are the downhole pressure $u_1 = \mathrm{PT1}_k$ and the wet christmas tree pressure $u_2 = \mathrm{PT2}_k$, and output $y_1 = \mathrm{TT2}_k$ is the wet christmas tree temperature.

Model validation for the observation models presented is shown in Figure 3c-d. The mean-absolute-percentual error (MAPE) of (7),(8), and (9) are 0,92%, 1,60%, and 1,77%, respectively.

5. EXPERIMENTAL RESULTS: STATE ESTIMATION

5.1 Linear versus Nonlinear Models

In order to recursively estimate the downhole pressure (PT1), we now use the identified models presented in Section 4. For the well $W1$, we combine the following pairs of models: i) $\{W1\_\hat{f}^1, W1\_\hat{h}^3\}$, ii) $\{W1\_\hat{f}^2, W1\_\hat{h}^2\}$ and iii) $\{W1\_\hat{f}^3, W1\_\hat{h}^1\}$ using UKF, iv) $\{W1\_\hat{f}^4, W1\_\hat{h}^4\}$, v) $\{W1\_\hat{f}^5, W1\_\hat{h}^5\}$, vi) $\{W1\_\hat{f}^6, W1\_\hat{h}^6\}$, vii) $\{W1\_\hat{f}^4, W1\_\hat{h}^6\}$ and viii) $\{W1\_\hat{f}^7, W1\_\hat{h}^7\}$ using KF. Henceforth, these eight schemes will be respectively referred as UKF1, UKF2, UKF3, KF1, KF2, KF3, KF4 and KF5. Combining the pairs of nonlinear models UKF1, UKF2 and UK3 using an IMM filter bank yields IMM NL1. The same was done to the pairs of affine models KF1, KF2 and KF3, yielding IMM L1. These pairs of models are chosen because they yield better performance compared to the other possible combinations (not shown) of process and observation models. Recall that seabed variables are used only in KF5.

Figure 4 illustrates downhole pressure estimation for the well W1 by the IMM NL1 and IMM L1 schemes. For convenience, data corresponding to a period of 7 months were divided into 9 windows. In Figure 4a, one can see an increasing drift in the measured $PT1$ data. This drift is expected for oil wells as they age. Though this drift is observed in the downhole pressure, it does not appear in any other process variable. Therefore, input data do not contain this information. Even though the process models are autoregressive, the drift's dynamics is too slow and cannot be captured during the modeling step with the chosen sampling period.

Still testing downhole pressure estimation for the well W1, Figure 5 illustrates the results for schemes KF4 and KF5. Measured data was the same as described for Figure 4.

In order to evaluate what is the gain of using nonlinear models compared to linear models while composing (U)KFs and IMM filter banks, we run tests using data from two wells, $W1$ and $W2$. The results for $W1$ are shown in in Figure 4. For $W2$, ten closed-loop schemes were tested. Five of them were assembled using the models described in Table 2 as: i) $\{W2\_\hat{f}^1, W2\_\hat{h}^1\}$, ii) $\{W2\_\hat{f}^2, W2\_\hat{h}^2\}$, iii) $\{W2\_\hat{f}^3, W2\_\hat{h}^1\}$ and iv) $\{W2\_\hat{f}^4, W2\_\hat{h}^2\}$ using KF, and v) combining the four pairs of models using an IMM filter bank. Henceforth, these five schemes will be respectively referred as KF6, KF7, KF8, KF9 and IMM L2. The other five schemes for $W2$ are the same used in (Teixeira et al., 2014) as UKF1, UKF2, UKF3, UKF4 and IMM and are not shown here for brevity. In this paper, for notational convenience, they will be referred as UKF4, UKF5, UKF6, UKF7 and IMM NL2. Note that only nonlinear models are used in scheme IMM NL2, while affine models are used in IMM L2. Figure 6 illustrates downhole pressure estimation for the well $W2$ by the IMM L2 and IMM NL2 schemes. Data were divided into 6 windows.

Copyright © 2015, IFAC

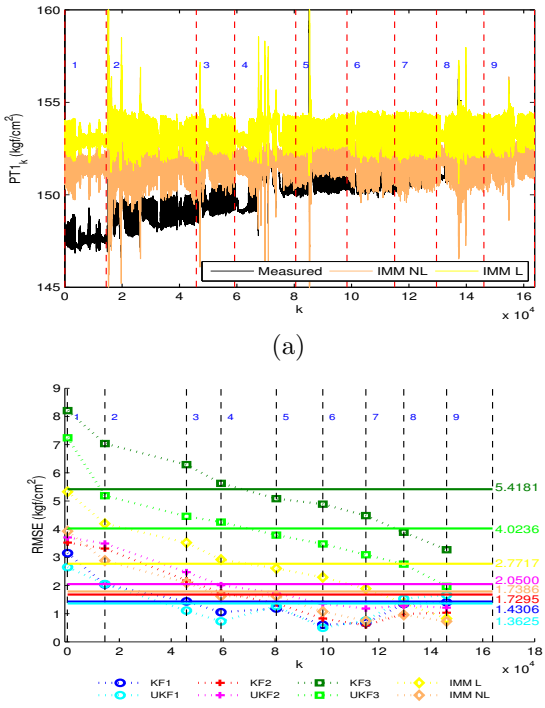

(a)

(b)

Fig. 4. (a) $W1$ downhole pressure estimation using IMM built with linear (IMM L1) and nonlinear (IMM NL1) models and (b) RMSE index (kgf/cm^2) calculated for each one of the 9 windows of data. Each point in the plot is the average RMSE for a window. The horizontal solid lines determines the average RMSE for the period of 7 months, while the vertical dashed lines determines the windows of data.

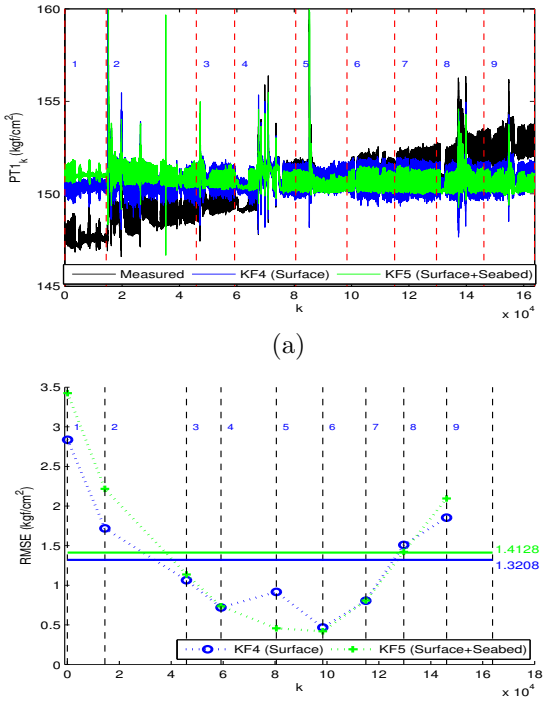

(a)

(b)

Fig. 5. (a) $W1$ downhole pressure estimation using $KF4$ and $KF5$, and (b) RMSE index (kgf/cm^2) calculated for each one of the 9 windows of data.

It is very important to note that, for comparison reasons, the models used in IMM L1 and IMM L2 were built to be affine versions of the nonlinear models composing IMM NL1 and IMM NL2, respectively. That is, we used the same input and output variables in the models and, whenever possible, the same modelling data. For example, process models $W1\_\hat{f}^4$ and $W1\_\hat{f}^5$ are affine versions of $W1\_\hat{f}^1$ and $W1\_\hat{f}^2$, respectively. The same applies to observation models, as $W1\_\hat{h}^4$ and $W1\_\hat{h}^5$ are linear versions of $W1\_\hat{h}^1$ and $W1\_\hat{h}^2$. Thus, this relation can be extended to the (U)KFs and IMM filter banks, being KF1 and IMM L1 linear versions of UKF1 and IMM NL1, respectively.

From figures 4 and 6, we see that the KFs and linear IMM filter banks (IMM L1 and IMM L2) were consistently beaten by their nonlinear counterparts, except for KF2 and KF8 which were better than UKF2 and UKF6, respectively. However, we see that the comparative performance of the aforementioned schemes was not significatively different. For $W1$, the largest difference between RMSE indexes occurred for KF3 and UKF3, with values of 5.41 kgf/cm^2 and 4.02 kgf/cm^2, respectively. Considering that PT1 varies in the range 145-160 kgf/cm^2 in this well, the improvement of UKF3 over KF3 may not pay off. Taking into account only the RMSE indexes obtained for IMM L1 and IMM NL1, 2.77 kgf/cm^2 and 1.73 kgf/cm^2, respectively, we see that the nonlinear scheme improved accuracy in about 1 kgf/cm^2.

Similar results were obtained for $W2$. RMSE indexes obtained for IMM L2 and IMM NL2 were 3.11 kgf/cm^2 and 1.54 kgf/cm^2, respectively, yielding accuracy improvement of 3.1% by the use of nonlinear models, considering that PT1 varies in the range 60-110 kgf/cm^2 in this well. Though nonlinear models yield better results when composing UKFs and IMM filter banks, the usage of linear and affine models seems to pay off. Besides, it is simpler to extend the structure of an affine model of a specific well to other wells, as well as to deal with the retuning of the models to address time-varying dynamics. Also, it is easier to guarantee global stability of affine models.

5.2 Platform versus Seabed process variables

Finally, in order to corroborate the results obtained in (Teixeira et al., 2014), we investigate what is the cost of using only platform process variables compared to the case in which seabed (specifically, wet christmas tree) variables are also assumed to be measured. Wet christmas tree variables are often highly correlated to downhole variables; however, their measurements are not always available.

We consider two wells to investigate this point: $W1$, whose results are shown in Figure 5, and $W3$ as follows. For the latter, two closed-loop schemes were tested: i) $\{W3\_\hat{f}^1, W3\_\hat{h}^1\}$ and ii) $\{W3\_\hat{f}^2, W3\_\hat{h}^2\}$ using KF, which will be referred as KF10 and KF11, respectively. Note that only platform variables are used in KF10, while seabed variables are used only in KF11. Figure 7 illustrates downhole pressure estimation for the well $W3$ using the KF10 and KF11 schemes. Data with duration of 7 months were divided into 7 windows,.

From Figures 5 and 7, one can see that KF4 and KF10 (that is, filters that use platform measurements) yield

Copyright © 2015, IFAC

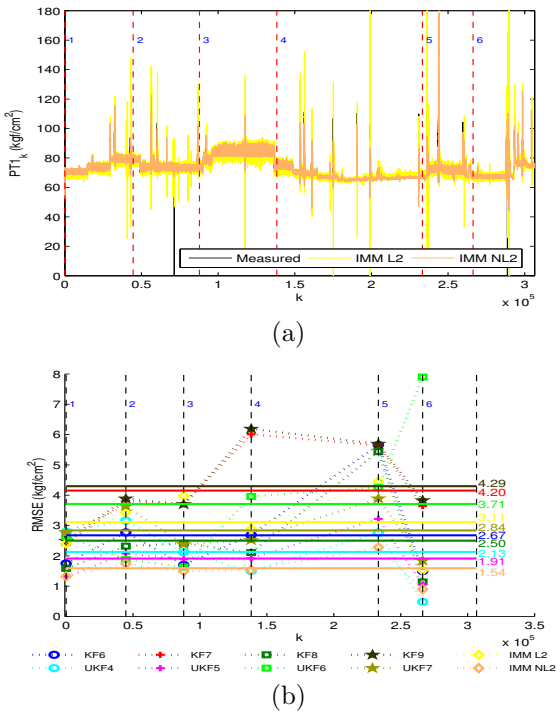

(a)

(b)

Fig. 6. (a) $W2$ downhole pressure estimation using IMM built with linear models (IMM L2) and IMM built with non-linear models (IMM NL2), and (b) RMSE index (kgf/cm^2) calculated for each one of the 6 windows of data.

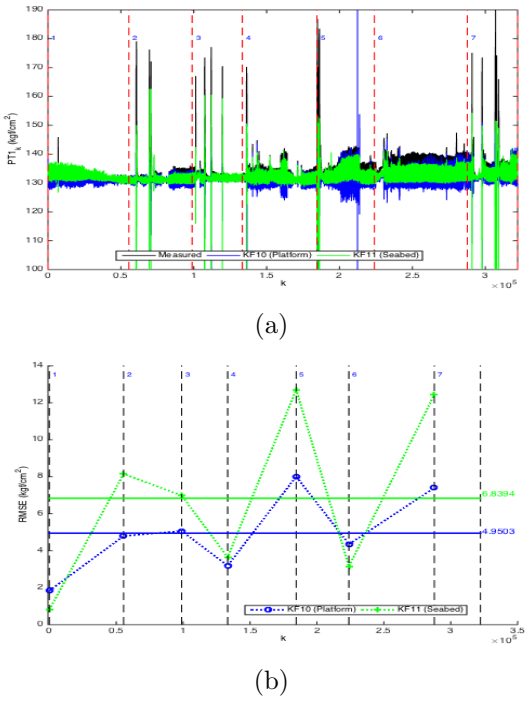

(a)

(b)

Fig. 7. (a) $W3$ downhole pressure estimation using $KF10$ and $KF11$, and (b) RMSE index (kgf/cm^2) calculated for each one of the 7 windows of data.

smaller RMSE indexes compared to KF5 and KF11. If we consider that PT1 varies in the range 145-160 kgf/cm^2 for well $W1$ and 120-180 kgf/cm^2 for well $W3$, using only platform variables improved accuracy in about 0.6% for the first and 3.1% for the last. Comparing to the results obtained in (Teixeira et al., 2014), where the use of seabed variables improved estimation in about 3.3%, it seems that measuring seabed variables is not critical for monitoring downhole pressure.

6. CONCLUDING REMARKS

The problem of designing data-driven soft sensors to estimate the downhole pressure in gas-lifted oil wells is investigated in this paper. Most soft sensors developed for gas-lift oil wells (reported in the literature) are model-driven and, thus, require the knowledge of physical parameters. We employ a two-step procedure, in which black-box models identified from historical data are used in interacting multiple model filter banks. That is, we perform closed-loop model prediction.

Experimental results suggest that the gain of using nonlinear models compared to affine models does not pay off. For the data tested, the largest difference between RMSE indexes from comparable nonlinear and linear schemes was 2.29 kfg/cm^2, for a well where the downhole pressure varies in the range 60-110 kgf/cm^2. Moreover, the usage of affine models has other advantages, such as simpler extension of structure from a specific well to another, as well as simpler model retuning to address time-varying dynamics.

Finally, we evaluated the advantage of measuring seabed process variables and using such measurements in state estimation. For the data tested in this paper, the small differences between the RMSE indices suggest that measuring seabed variables is not critical to monitor downhole pressure.

REFERENCES

L.A. Aguirre. A nonlinear correlation function for selecting the delay time in dynamical reconstructions. *Physics Letters A*, 203(2-3): 88-94, 1995.

L.A. Aguirre, B.O.S. Teixeira, and L.A.B. Tôrres. Using data-driven discrete-time models and the unscented Kalman filter to estimate unobserved variables of nonlinear systems. *Physical Review E*, 72(2): 026226, 2005.

Y. Bar-Shalom, X. R. Li, and T. Kirubarajan. *Estimation with Applications to Tracking and Navigation*, Wiley-Interscience, New York, USA, 2001.

E. Domlan, B. Huang, F. Xu, and A. Espejo (2011). A decoupled multiple model approach for soft sensors design. *Control Engineering Practice*, 19: 126–134.

J. Eck, U. Ewherido, et al. (1999). Downhole Monitoring: The Story So Far. *Oilfield Review*, 11(4): 20–33.

K. Fujiwara, M. Kano, and S. Hasebe (2012). Development of correlation-based pattern recognition algorithm and adaptive soft-sensor design. *Control Engineering Practice*, 20: 371–378.

L. Fortuna, S. Graziani, A. Rizzo, and M.G. Xibilia. *Soft Sensors for Monitoring and Control of Industrial Processes*, Springer, 2007.

P. Kadlec, B. Gabrys, and S. Strandt. Data-driven soft sensors in the process industry. *Computers and Chemical Engineering*, 33(4): 795–814, 2009.

D.J. Pagano, V. Dallagnol Filho and A. Plucênio (2006). Identification of Polinomial NARMAX Models for an Oil Well Operating by Continuous Gas-Lift. *IFAC Intern. Symp. on Advanced Control of Chemical Processes*, Gramado, Brazil, 1113–1118.

B.O.S. Teixeira, W.S. Castro, A.F. Teixeira and L.A. Aguirre. Data-driven soft sensor of downhole pressure for a gas-lift oil well. *Control Engineering Practice*, 22(1): 34–43, 2014.

H. Yang, R. Lu, K. Zhang and X. Wang. Multiple Model Predictive Control of Component Content in Rare Earth Extraction Process. *Journal of Computers*, 7(10): 2557–2563, 2012.

Copyright © 2015, IFAC